CH-09-017

Determining Off-Normal Solar Optical Properties of Roller Blinds

Nathan A. Kotey
Student Member ASHRAE

John L. Wright, PhD, PEng
Member ASHRAE

Michael R. Collins, PhD
Associate Member ASHRAE

ABSTRACT

Solar gain through fenestration constitutes a significant portion of peak cooling load and annual energy consumption in buildings. As such, any reduction in solar gain translates into savings associated with the cost of purchasing and operating cooling equipment. Shading devices in general, and roller blinds in particular, can be used to reduce solar gain appreciably. The performance of a roller blind is largely determined by its solar optical properties. In this study, an integrating sphere was used to obtain off-normal solar properties of six typical roller blind samples. Measurements were used to develop semi-empirical models for the off-normal beam-beam, beam-diffuse, and diffuse-diffuse solar optical properties. The models provide a means to calculate off-normal properties by adjusting known values of beam-beam transmittance (i.e., openness), beam-total transmittance, and beam-total reflectance measured at normal incidence. The properties that apply to normal incidence are readily obtained. Such models are valuable components of building energy simulation software.

INTRODUCTION

The capability of window shading devices—roller blinds in particular—to reduce solar heat gain through windows has been an important research topic for many years. The ability to accurately quantify the reduction in cooling load that these devices deliver would be an asset to architects, engineers, and building designers in general.

Several studies have shown that roller blinds can significantly reduce energy costs associated with windows. Grasso and Buchanan (1979, 1982) reported a 60% reduction in energy costs when a light-coloured opaque roller blind was used during the cooling season. A light-coloured translucent roller blind yielded an annual cost reduction of 50%. During the heating season, they found that roller blinds had the potential of reducing energy cost since they reduce heat transfer through the window. For climates with net seasonal energy loss, an average of 34% reduction in energy cost was realised when conventional roller blinds were attached to a window. They also noted that the percentage reduction in the energy cost during the heating season was insensitive to the type and colour of the roller blind used but was sensitive to the proximity of the roller blind to the window—the roller blinds tended to be more effective in reducing heat transfer when installed closer to the window. The energy saving potential of roller blinds has also been examined by means of calorimetric measurements (e.g., Ozisik and Schutrum [1959], Grasso and Buchanan [1982], and Harrison and van Wonderen [1998]). Such measurements are time consuming and expensive.

With the advent of several computational techniques, the energy saving potential of roller blinds can be readily calculated if the solar optical and the thermal properties of individual layers of a glazing/shading system are known (e.g., Wright and Kotey [2006], EnergyPlus [DOE 2007], and van Dijk et al. [2002]). The procedure takes advantage of the fact that there is no appreciable overlap between the solar and the longwave radiation bands. This leads to a two-step analysis. First, solar radiation models determine the fraction of incident solar radiation that is directly transmitted and the fraction that is absorbed in each layer of the glazing system. The solar radiation absorbed in each layer then serves as a source term in the second step—the heat transfer analysis. For building energy simulation, the two-step analysis is done on a time-step basis. Since the location of the sun and therefore the incidence angle, θ, changes by the hour, solar optical properties of the individ-

Nathan A. Kotey is a graduate student, **John L. Wright** is a professor, and **Michael R. Collins** is an associate professor in the Department of Mechanical and Mechatronics Engineering, University of Waterloo, Waterloo, Ontario, Canada.

ual layers of any glazing/shading system must be available for any given angle of incidence.

Solar optical properties of glazings, including coated and tinted glazings, can readily be estimate at any given value of θ (e.g., Furler [1991], Pfrommer et al. [1995], Roos [1997], and Rubin et al. [1998, 1999]). The off-normal solar optical properties of roller blinds, however, are not readily available. Normal incidence solar optical properties are easily obtained, however, and a means of estimating the off-normal and diffuse properties from these is highly desirable.

Shading layers are often characterised by making the assumption that each layer, whether homogeneous or not, is represented by an equivalent homogenous layer with spatially averaged "effective" optical properties (e.g., Parmelee and Aubele [1952], Farber et al. [1963], Pfrommer et al. [1996], and Yahoda and Wright [2005]). Such an approach has been shown to provide accurate characterisation of venetian blinds (e.g., Kotey et al. [2008]).

Careful consideration of solar radiation incident on a shading layer with some openness reveals that some portion of the radiation passes undisturbed through openings while the remaining portion is intercepted by the structure of the layer. The structure may consist of yarn, slats, or some other material. A portion of the intercepted radiation is absorbed and the rest is scattered, leaving the layer as an apparent reflection or transmission. These scattered components are assumed to be uniformly diffuse.

The use of effective optical properties and a beam/diffuse split of solar radiation at each layer of a multilayer system provides virtually unlimited freedom to consider different types of shading layers. This approach also delivers the high computational speed needed in building energy simulation tools.

A recent study by Kotey et al. (2009a) used specially designed sample holders attached to an integrating sphere of a commercially available spectrophotometer to measure the off-normal solar optical properties of drapery fabrics. The integrating sphere is particularly useful since it can separate the undisturbed and scattered components of incident beam radiation. Kotey et al. measured the spectral beam-beam transmittance, beam-diffuse transmittance, and beam-diffuse reflectance at incident angles ranging from 0 to 60° and then calculated the corresponding solar properties (ASTM 1996). Having obtained the solar properties at varying θ, cosine power functions were fitted to normalised forms of the measured data. The cosine power function was chosen because it is symmetrical about $\theta = 0$. Furthermore, the shape of the function can be modified by adjusting the exponent, or it can be scaled to a cutoff angle where transmission falls to zero. Given the solar optical properties of any fabric at normal incidence, the proposed semi-empirical models can be used to calculate the corresponding off-normal properties. Properties that apply to diffuse insolation can also be obtained. The same experimental procedure and approach to model development were adopted in this study of roller blinds.

PRELIMINARY CONSIDERATIONS

The roller blind samples considered in this study have a general structure similar to drapery fabrics (e.g., Kotey et al. [2009a]). A typical roller blind is made up of strands of yarn may be woven loosely, leaving open areas, or woven tightly, with no open areas. There are subtle differences, however, in the material composition of roller blinds and drapery fabrics. The roller blind material, for example, is usually made from two or more layers of vinyl, fibreglass, PVC, and/or polyester. As such, it appears to be more rigid in comparison with drapery fabric, which is typically made from softer materials such as cotton, wool, silk, etc. The differences in material composition generally translate into differences in optical characteristics.

When beam radiation is incident on the surface of a roller blind, it is split into two portions: the undisturbed portion transmitted through the openings, and the intercepted portion—some of which will be scattered in the forward direction (i.e., transmitted) or scattered in the reverse direction (i.e., reflected). The scattered components, regardless of their true directional nature, are categorised as purely diffuse. This is done because the models presented here will be used within a multilayer glazing/shading model where beam and diffuse components of solar radiation are tracked (Wright and Kotey 2006). The undisturbed portion constitutes the beam-beam (specular) transmittance, τ_{bb}. At normal incidence, τ_{bb} is equivalent to the openness factor, $A_o = \tau_{bb}(\theta = 0)$, defined as the ratio of the open area to the total area of the material. The intercepted radiation is scattered by multiple reflections between (and possible transmission through) the strands of yarn. The portion of the intercepted radiation that is not absorbed by the yarn subsequently emerges in the forward direction as beam-diffuse transmittance, τ_{bd}, or in the backward direction as beam-diffuse reflectance, ρ_{bd}. The beam-total transmittance, τ_{bt}, is the sum of τ_{bb} and τ_{bd}. Preliminary reflectance measurements show that roller blinds generally have negligible specular component; hence, the beam-beam (specular) reflectance, ρ_{bb}, is zero. The beam-total reflectance is therefore equal to the beam-diffuse reflectance: $\rho_{bt} = \rho_{bd}$. Incident diffuse radiation remains diffuse in transmission or reflection, and the corresponding diffuse-diffuse properties are τ_{dd} and ρ_{dd}.

EXPERIMENTS

Test Samples

The roller blinds tested were grouped into two categories: open and closed weave. In all, six different samples were considered (see Figure 1):

1. Open weave, vinyl coated fibreglass, both sides white, thickness 0.55 mm, A_o = 14%.

2. Open weave, vinyl coated fibreglass, both sides black, thickness 0.55 mm, A_o = 14%.
3. Open weave, 25% polyester, 75% PVC on polyester, both sides chalk, thickness 0.80 mm, A_o = 5%.
4. Open weave, 25% polyester, 75% PVC on polyester, both sides ebony, thickness 0.80 mm, A_o = 5%.
5. Closed weave, 12 oz fibreglass, opaque, duplex, room darkening, one side black one side white, thickness 0.33 mm, A_o = 0.
6. Closed weave, 84% polyester, 16% linen, translucent, both sides natural glacier, thickness 0.35 mm, A_o = 0.

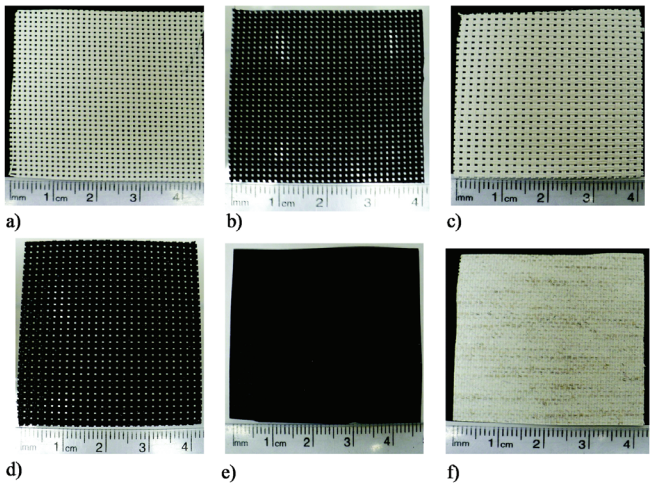

Figure 1 *Roller blind samples: a) White_14%, b) Black_14%, c) Chalk_5%, d) Ebony_5%, e) Duplex_black side, and f) glacier.*

Instrumentation

A commercially available spectrophotometer was used in this study. It is a double beam, direct ratio recording, rapid scanning instrument with a resolution of less than 0.05 nm for ultraviolet and visible spectra (UV-VIS) and less than 0.2 nm for the near infrared (NIR) spectrum; its repeatability characteristics are less than 0.025 nm for UV-VIS and less than 0.1 nm for NIR. It has an extended spectral range allowing it to scan between wavelengths of 0.17 and 3.30 μm. An integrating sphere (IS) accessory was mounted in the spectrophotometer to measure reflectance and transmittance of samples with appreciable scattering characteristics. The IS is particularly useful since it can resolve the undisturbed and scattered components of incident beam radiation. The sphere is hollow and its inner surface is coated with polytetrafluoroethylene with a high and uniformly diffuse reflectance. In theory, any light entering the sphere is uniformly distributed over the entire inner surface. A radiation detector on the sphere wall receives an integrated signal. A detailed description of the IS as well as the different components of transmittance and reflectance measurements that can be obtained with the sphere are discussed in the study by Kotey et al. (2009a).

To measure off-normal solar optical properties, fixed sample holders were attached to the IS as shown in Figures 2a and 2b. The sample holders were made from aluminium tubes with one end machined at a known angle, θ , ranging from 0° to 60° in 15° steps. When installed in the transmission or the reflection port, the sample holder projected into the IS and its length was such that it allowed only the angled portion to protrude into the sphere. The exterior surface of each sample holder was highly polished to reflect incident radiation and retain the high response of the sphere. On the other hand, the

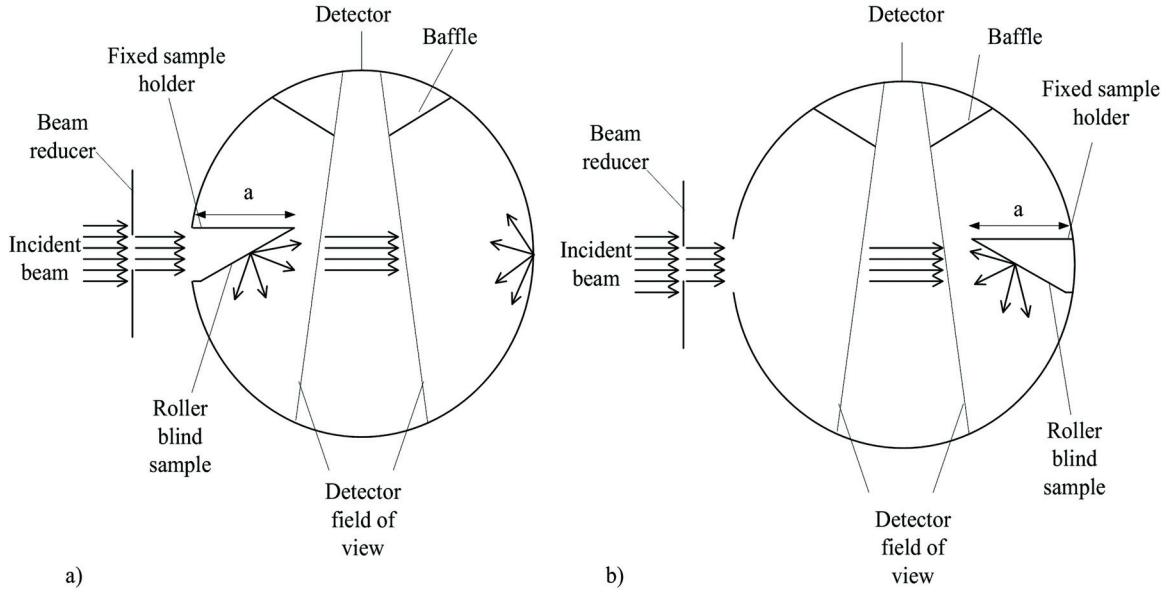

Figure 2 *a) Off-normal transmittance measurement and b) off-normal reflectance measurement.*

interior surface of each tube was painted black in order to absorb radiation scattered in reflection during a transmittance measurement or scattered in transmission during a reflectance measurement. The sample holders were mounted at the ports of the IS with the aid of machined adapters. Each adapter is an aluminium block with a hole at its centre. At the transmission port, the incident beam is wider than the inner diameter of the the sample holder. To ensure that the incident beam passed through the sample holder without any interference, a beam reducer was glued to the face of the transmission adapter. The beam reducer is simply a thin aluminium plate with a hole slightly smaller than the inner diameter of the tubular sample holders. A set of reflectance references were also fabricated for calibrating the sphere. They were made by filling the angled end of sample holders with barium sulphate paste. This formed a smooth reflectance surface having the same end angle as the sample holders.

To measure off-normal solar optical properties without using the IS, a rotatable sample holder was fabricated. It allowed the spectrophotometer to measure beam-beam transmittance at θ ranging from 0° to 80°. Measurements with a rotatable sample holder were particularly useful since they served the purpose of validating the measurements obtained with the IS and also gave some information on the transmittance at grazing angles of incidence.

Transmittance Measurements with the IS

The IS was installed in the spectrophotometer. A fixed sample holder without any sample attached was mounted at the transmission port while the apparatus was calibrated. Subsequently, a roller blind sample was attached to the angled end of the holder and mounted at the transmission port as shown in Figure 2a. Spectral beam-total transmittance measurements were then obtained with the reflection port closed. Without moving the sample, the reflection port was opened and spectral beam-diffuse transmittance measurements were taken. The difference between the two sets of readings gave the spectral beam-beam transmittance of the sample. Spectral transmittance measurements of the other samples were subsequently taken. The entire process was repeated with another fixed sample holder with a different end angle.

Transmittance Measurements without the IS

The IS was replaced with a transmittance tray that had the rotatable sample holder installed. The spectrophotometer was calibrated. A roller blind sample was then attached to the rotatable sample holder and the spectral beam-beam transmittance subsequently taken at $\theta = 0°, 15°, 30°, 45°, 60°, 70°$, and 80°. Without recalibrating the instrument, the measurement process was repeated for the other samples.

Reflectance Measurements with the IS

The IS was installed in the spectrophotometer. A reflectance reference with an end angle, θ, was mounted at the reflectance port. The transmission adapter was also mounted to reduce the size of the incident beam. The instrument was subsequently calibrated. The reflectance reference was replaced with a sample holder having a sample attached as shown in Figure 2b. The spectral beam-diffuse reflectance measurements were then taken. The measurement process was repeated with other roller blind samples. Having obtained spectral measurements for all samples at θ, the calibration and measurement process was repeated for other sample holders with different values of θ.

Calculation of Solar Properties

The solar properties at any given θ were calculated from spectral measurements using the 50-point selected ordinate method as described in ASTM E903-96 (ASTM 1996). The solar irradiance distribution (ASTM 1987) was divided into 50 wavelength intervals, each containing 1/50 of the total irradiance. The spectral optical property was then evaluated at the centroidal wavelength of each interval.

Uncertainty

Measurements were done in accordance with ASTM E903-96 (ASTM 1996). This standard quotes an expected uncertainty of ±2%, with most of this uncertainty arising from the conversion of spectral data to integrated solar properties. A more conservative estimate of uncertainty, ±3%, was used in this study, with the additional uncertainty arising from the use of the sample holders (the use of barium sulphate for calibration, the reduction in beam size, and the projection and orientation of the holders in the IS). Special care was taken to minimise errors arising from the use of the sample holders. More detail can be found in the study by Kotey et al. (2009a).

SEMI-EMPIRICAL MODELS

Beam-Total Reflectance Model

For each sample considered, a plot of ρ_{bt} versus θ revealed an insignificant variation of ρ_{bt} with respect to θ (see Figure 3). In the absence of measurements at $\theta > 60°$, and noting that the reflectance of a rough surface might realistically be independent of incidence angle, the beam-total reflectance is considered to be constant:

$$\rho_{bt}(\theta) = \rho_{bt}(\theta = \theta) \tag{1}$$

Beam-Beam Transmittance Model

The measured values of τ_{bb} were normalised according to the definition shown in the left-hand section of Equation 2:

$$^{norm}\tau_{bb} = \frac{\tau_{bb}(\theta)}{\tau_{bb}(\theta = \theta)} = \cos^{b}\left(\frac{\theta}{\theta_{cutoff}} \cdot \frac{\pi}{2}\right) \qquad \theta \le \theta_{cutoff} \tag{2}$$

The resulting values of $^{norm}\tau_{bb}$ are shown in Figure 4. It was observed that τ_{bb} diminished to zero at $\theta \approx 65°$ in each case. Measurements carried out by Look (1986) on three different awning fabrics with $A_o = 6\%$ also revealed that τ_{bb} fell to zero

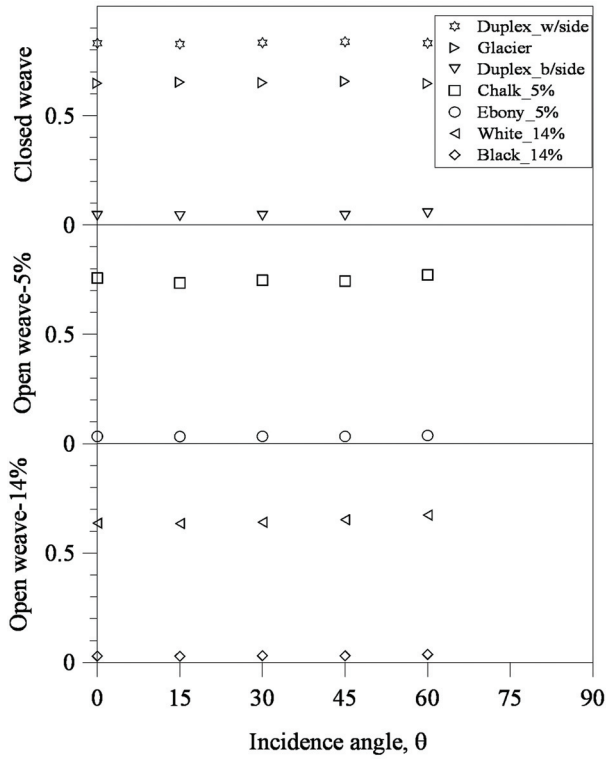

Figure 3 *Beam-total reflectance versus incidence angle.*

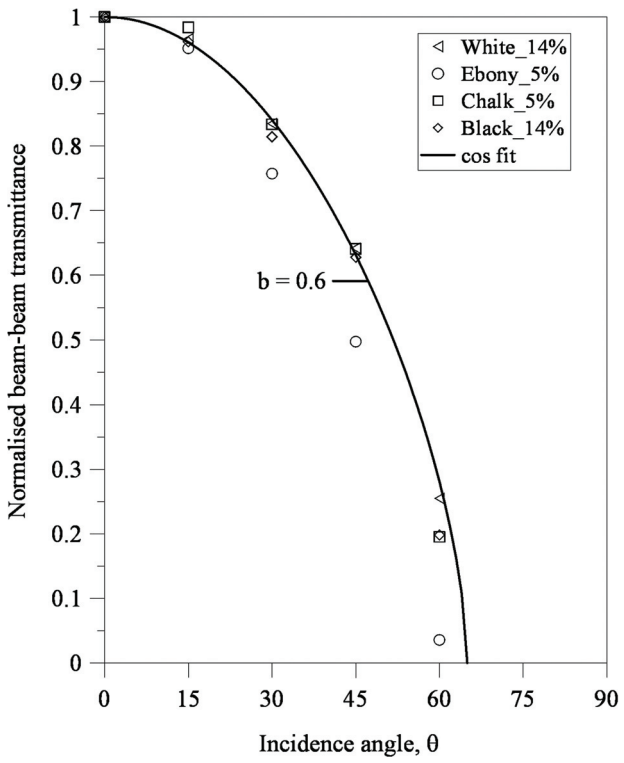

Figure 4 *Normalised beam-beam transmittance versus incidence angle.*

at $\theta \approx 65°$. Two parameters, θ_{cutoff} and b, as shown in Equation 2, were used to characterise off-normal beam-beam transmission through all roller blind materials. As seen in Figure 4, by choosing $b = 0.6$ and $\theta_{cutoff} \approx 65°$, Equation 2 closely represents the measurements. However, it should also be recognised that as A_o approaches unity, as the structure of the roller blind disappears, the requirements that $b \to 0$ and $\theta_{cutoff} \to 90°$ must be satisfied to obtain 100% transmission and to remove any influence of incidence angle in this limit. Noting also that b and θ_{cutoff} do not vary appreciably in the range over which measurements were performed, $0 \le A_o \le 0.14$, Equations 3 and 4 are proposed:

$$b = 0.6\cos^{0.3}\left(A_o\frac{\pi}{2}\right) \tag{3}$$

$$\theta_{cutoff} = 65° + (90° - 65°)\cdot\left(1 - \cos\left(A_o\frac{\pi}{2}\right)\right) \tag{4}$$

Several points can be made regarding Equations 3 and 4:

1. In choosing a value for the exponent, b, little emphasis was placed on the data for the ebony sample because b will have virtually no influence on the calculation of $\tau_{bb}(\theta)$ for roller blind materials with such low solar transmission ($\tau_{bb}(\theta = 0) = 0.06$).
2. The exponent used in Equation 3 was chosen to ensure that τ_{bd} remains greater than zero for all values of A_o and θ (i.e., $\tau_{bt}(\theta) \ge \tau_{bb}(\theta)$ must always be true). This condition would be violated for materials where $\tau_{bb}(\theta = 0)$ approaches $\tau_{bt}(\theta = 0)$ if a larger exponent were used.
3. The exponent used in Equation 4 (i.e., unity) is based on measurements from a companion study (Kotey et al. 2009b) about insect screens where values of $\tau_{bb}(\theta)$ were available at much higher values of A_o.

Beam-Total Transmittance Model

Figure 5 shows the beam-total transmittance measurements, normalised according to the left-hand portion of Equation 5:

$$^{norm}\tau_{bt} = \frac{\tau_{bt}(\theta)}{\tau_{bt}(\theta = 0)} = \cos^{b}(\theta) \qquad \theta \le \theta_{cutoff} \tag{5}$$

When one examines Figure 5, it appears that a cutoff angle is needed near $\theta = 65°$, but only for the dark-coloured samples. However, a cutoff angle was not used. This decision was made for two reasons. First, some diffuse transmission can be expected, however small, as $\theta \to 90°$ for every roller blind material. Second, dark samples create very little scattered reflection or transmission. Therefore, there is some freedom to place more emphasis on the data for light-coloured samples.

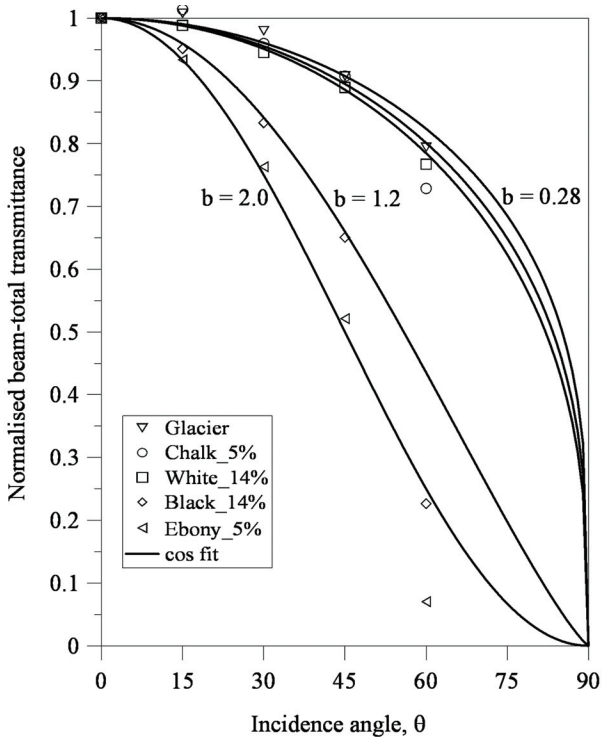

Figure 5 *Normalised beam-total transmittance versus incidence angle.*

The beam-total transmittance will be influenced not only by A_o (this influence is clearly seen in the model for $\tau_{bb}(\theta)$) but also by the way in which the structure of the material transmits solar radiation. Thus, noting that the portion of incident radiation intercepted by the structure is $1 - A_o = 1 - \tau_{bb}(\theta = 0)$ and also noting that the structure only produces diffuse transmission, the apparent transmittance of the roller blind structure, τ^{str}, is defined:

$$\tau^{str} = \frac{\tau_{bd}(\theta = 0)}{A_o} = \frac{\tau_{bt}(\theta = 0) - \tau_{bb}(\theta = 0)}{1 - \tau_{bb}(\theta = 0)} \tag{6}$$

An expression for b was developed by choosing $b \approx 2$ for values of τ^{str} corresponding to the dark roller blind samples and $b \approx 0.4$ for values of τ^{str} corresponding to the light roller blind samples. Recalling also that as A_o approaches unity we expect $b \to 0$, Equations 7a and 7b were developed:

$$b = 0.133(\tau^{str} + 0.003)^{-0.467} \qquad 0 \le \tau^{str} \le 0.33 \tag{7a}$$

$$b = 0.33(1 - \tau)^{str} \qquad (0.33 < \tau^{str} \le 1) \tag{7b}$$

In formulating Equation 7a, little emphasis was placed on the data for the two dark-coloured samples measured at $\theta = 60°$. This can be seen in Figure 5. This was done because b will have virtually no influence on the calculation of $\tau_{bt}(\theta)$ for roller blind materials with such low solar transmission, particularly at higher values of θ.

Beam-Diffuse Transmittance Model

At any given value of θ, the beam-diffuse transmittance is the difference between the beam-total and beam-beam transmittance values:

$$\tau_{bd}(\theta) = \tau_{bt}(\theta) - \tau_{bb}(\theta) \tag{8}$$

Diffuse-Diffuse Transmittance and Reflectance Models

The solar optical properties for incident diffuse radiation can be obtained by integrating the beam-total properties over the hemisphere. The diffuse-diffuse transmittance and reflectance are respectively given by

$$\tau_{dd} = 2 \int_0^{\pi/2} \tau_{bt}(\theta) \cdot \cos(\theta) \cdot \sin(\theta) d\theta \tag{9}$$

and

$$\rho_{dd} = 2 \int_0^{\pi/2} \rho_{bt}(\theta) \cdot \cos(\theta) \cdot \sin(\theta) d\theta \tag{10}$$

Noting that ρ_{bt} is taken to be constant for any given roller blind material, Equation 10 reduces to

$$\rho_{dd} = \rho_{bt}(\theta = 0) \tag{11}$$

Equation 9 can be evaluated using computational numerical methods.

RESULTS AND DISCUSSION

The solar optical properties measured at normal incidence are summarised in Table 1. The data include measurements made with and without the IS. Several observations can be made.

1. The two sets of $\tau_{bb}(\theta = 0)$ measurements, with and without the IS, agree to within ±0.01 even though τ_{bb} must be indirectly measured as the difference between τ_{bt} and τ_{bd} when the IS is used. This observation strengthens confidence in the validity of the measurements.
2. The openness factor, A_o, reported by the manufacturer closely matches the experimentally determined $\tau_{bb}(\theta = 0)$.
3. Generally, the light-coloured roller blinds have high values of $\rho_{bt}(\theta = 0)$ while the dark-coloured roller blinds exhibit very low values of $\rho_{bt}(\theta = 0)$. Since reflection and diffuse transmission are attributed primarily to multiple reflections within the structure of the material, a connection can be observed between $\tau_{bt}(\theta = 0)$ and $\rho_{bt}(\theta = 0)$ for roller blind materials with non-zero transmission.

Table 1. Summary of Measured Solar Optical Properties at Normal Incidence

Identification	Manufacturer's Reported Openness	Classification	Measurements With IS				Measurements Without IS
			Beam-Total Reflectance	Beam-Total Transmittance	Beam-Diffuse Transmittance	Beam-Beam Transmittance	Beam-Beam Transmittance
White_14%	0.14	Open weave	0.64	0.30	0.17	0.13	0.14
Black_14%	0.14	Open weave	0.03	0.13	0.01	0.12	0.12
Chalk_5%	0.05	Open weave	0.75	0.16	0.08	0.08	0.09
Ebony_5%	0.05	Open weave	0.03	0.07	0.01	0.06	0.07
Duplex_opaque (black side)	0.00	Closed weave	0.05	0.00	0.00	0.00	0.00
Duplex_opaque (white side)	0.00	Closed weave	0.84	0.00	0.00	-0.00	0.00
Glacier_ translucent	0.00	Closed weave	0.65	0.24	0.24	0.00	0.00

Table 2. Comparison Between Beam-Beam Transmittance Measurements With and Without the IS

Incidence Angle	White_14%			Black_14%			Chalk_5%			Ebony_5%		
	With IS	Without IS	Diff	With IS	Without IS	Diff	With IS	Without IS	Diff	With IS	Without IS	Diff
0	0.14	0.13	0.01	0.12	0.12	0.00	0.09	0.08	0.01	0.07	0.06	0.01
15	0.14	0.13	0.01	0.12	0.11	0.01	0.08	0.08	0.00	0.06	0.06	0.00
30	0.12	0.11	0.01	0.11	0.10	0.01	0.07	0.07	0.00	0.05	0.05	-0.00
45	0.11	0.09	0.02	0.08	0.07	0.01	0.05	0.05	0.00	0.03	0.03	-0.00
60	0.05	0.03	0.02	0.04	0.02	0.02	0.02	0.02	0.00	0.00	0.00	0.00

A comparison between τ_{bb} measurements, obtained with and without the IS, at various angles of incidence is shown in Table 2. The differences between the two sets of measurements are also listed (*Diff* columns). With a maximum difference of 0.02, the two sets of measurements agree within experimental uncertainty. Again, this agreement adds confidence in the instrument and calibration procedure.

Turning to the effect of θ, plots of τ_{bb}, τ_{bt}, and τ_{bd} are shown in Figures 6, 7, and 8, respectively. Each plot includes measured data points plus lines representing the semi-empirical models developed in this study. Each figure is subdivided according to openness in order to display overlapping results more clearly.

$\tau_{bb}(\theta)$ consistently decreases as θ increases, as is shown in Figure 6. Clearly, there is good agreement between the model and the measurements, to some extent because τ_{bb} is always small. Note the cutoff angle, $\theta_{cutoff} \approx 65°$. The data for closed weave roller blinds $(\tau_{bb}(\theta) = 0)$ are not shown in Figure 6.

Figure 7 shows beam-total transmission data. Again close agreement between measurement and the semi-empirical model is demonstrated. Also shown in Figure 7 are the error bars representing the uncertainty for measurements made with the Black_14% sample. For all roller blinds, τ_{bt} decreases as θ increases.

The variation of τ_{bd} with θ shows an interesting trend among the various roller blinds as seen in Figure 8. For the closed weave roller blind with $\tau_{bb} = 0$, τ_{bd} is simply equal to τ_{bt} and decreases with an increase in θ. The light-coloured open weave roller blinds (White_14% and Chalk_5%) have similar beam-diffuse characteristics. They both show a gradual increase in τ_{bd} to a maximum value before decreasing as θ increases. Little can be said about dark-coloured open weave roller blinds (Black_14% and Ebony_5%) with very small values of τ_{bd} over the entire range of θ.

The test samples used in this study represent the range of products used in common practice. However, these samples all have relatively little openness, $A_o \leq 14\%$, and some restrictions may apply to the models presented here. For example, it

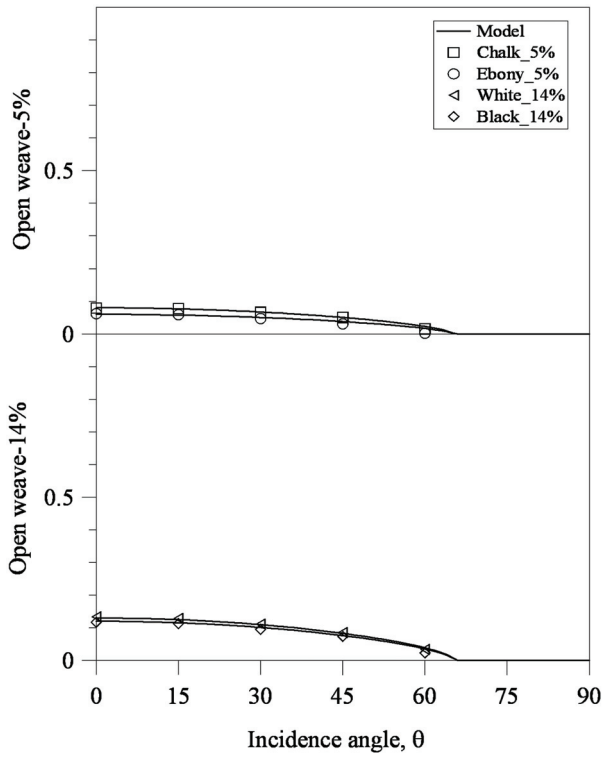

Figure 6 *Beam-beam transmittance versus incidence angle.*

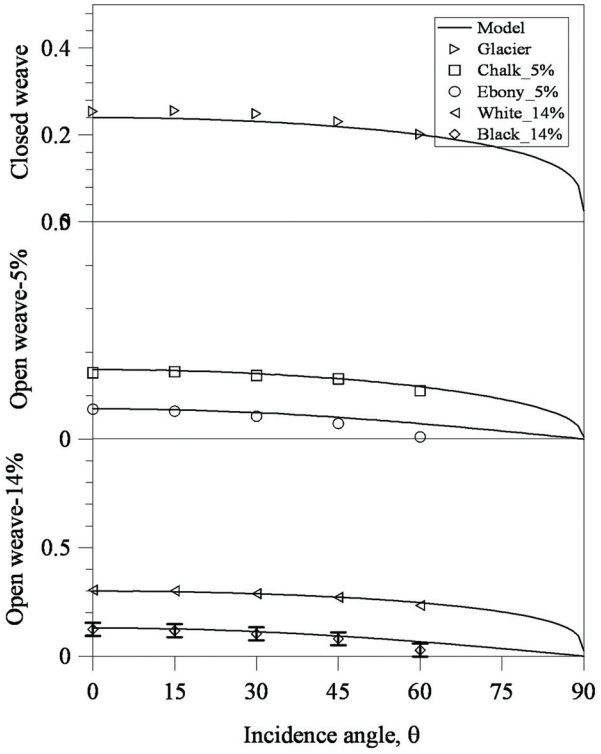

Figure 7 *Beam-total transmittance versus incidence angle.*

is clear that Equation 2 can safely be used for small values of A_o, say $A_o \leq 20\%$, and for the unlikely situation of large values of A_o, say $A_o > 80\%$ (because of the limits accommodated by Equations 3 and 4), but some uncertainty can be expected at intermediate values of A_o.

Finally, it should be noted that all of the non-opaque test samples were optically symmetric. The models presented here are trivial when used to characterise opaque roller blinds (zero transmission and constant reflectance) and therefore can be safely applied to asymmetric materials such as the black/white material included in this study (sample e from Figure 1). In contrast, it is not clear how well the models apply to asymmetric materials that allow some diffuse transmission. This is not a serious limitation. Certainly the current models will work well for asymmetric materials that have little diffuse transmission ($\tau_{bt}(\theta = 0) \approx \tau_{bb}(\theta = 0)$). Regardless, the vast majority of roller blinds are optically symmetric. The extension of the current models, if necessary at all, will be the subject of future research.

CONCLUSIONS

This study presents a set of models for generating off-normal solar optical properties of roller blinds. The models provide a means to calculate off-normal properties by adjusting known values of beam-beam transmittance (i.e., openness), beam-total transmittance, and beam-total reflectance

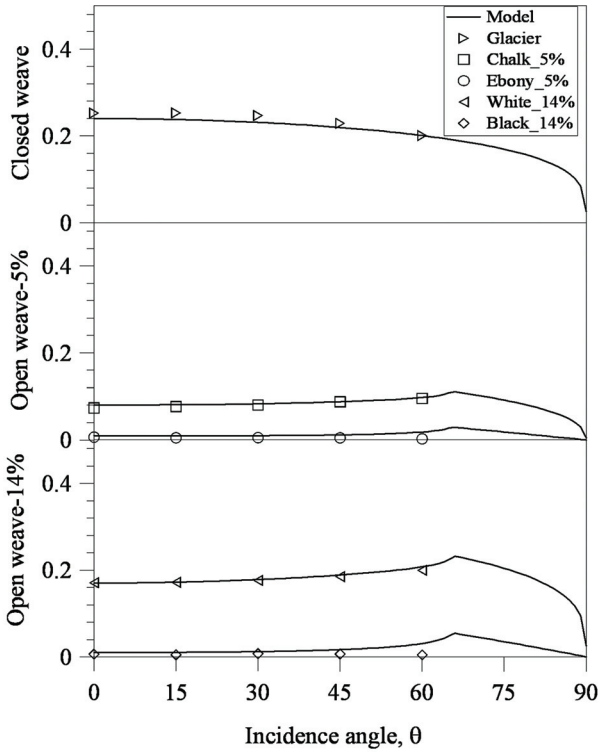

Figure 8 *Beam-diffuse transmittance versus incidence angle.*

measured at normal incidence. The properties that apply to normal incidence are readily obtained and are the same properties used to characterise drapery materials as seen in Keyes's chart (Keyes 1967; ASHRAE 2005). These models are based on experiments made with special sample holders attached to an integrating sphere of a commercially available spectrophotometer. Measurement results for six roller blind materials are reported. The measurements show that roller blind reflectance includes no specular component and no variation of reflectance was observed with respect to incidence angle, at incidence angles within 60° of normal. On the other hand, the variation of roller blind transmittance with incidence angle was observed and can be represented by a cosine power function. Models for roller blind transmittance were obtained by fitting curves that closely matched the experimental data. Given solar optical properties obtained at normal incidence, the proposed semi-empirical transmittance models can be used to characterise the off-normal transmittance of any roller blind, including blinds with a moderate amount of openness. The off-normal models can be integrated to obtain the diffuse properties. The models have also been formulated so that they can be applied to both optically symmetric and asymmetric roller blind materials. This set of models provides significant potential as a component of building simulation software, for calculating both peak cooling load and energy consumption.

ACKNOWLEDGMENTS

We would like to thank Natural Sciences and Engineering Research Council and ASHRAE 1311-TRP for financial support and Shade-O-Matic for supplying the roller blind samples.

NOMENCLATURE

Symbols

A_o = openness
b = exponent
ρ = reflectance (dimensionless)
τ = transmittance (dimensionless)
θ = incidence angle

Subscripts

b = back surface
bb = beam-beam
bd = beam-diffuse
bt = beam-total
cutoff = cutoff angle
dd = diffuse-diffuse
f = front surface

Superscripts

str = structure
norm = normalised

REFERENCES

ASHRAE. 2005. *2005 ASHRAE Handbook—Fundamentals*. Atlanta: American Society of Heating, Refrigerating and Air-Conditioning Engineers, Inc.

ASTM 1987. *ASTM E891-87, Standard Tables for Terrestrial Direct Normal Solar Spectral Irradiance for Air Mass 1.5*. Philadelphia: American Society for Testing and Materials.

ASTM. 1996. *ASTM E903-96, Standard Test Method for Solar Absorptance, Reflectance, and Transmittance of Materials Using Integrating Spheres*. Philadelphia: American Society for Testing and Materials.

Farber, E.A., W.A. Smith, C.W. Pennington, and J.C. Reed. 1963. Theoretical analysis of solar heat gain through insulating glass with inside shading. *ASHRAE Journal* pp. 79.

Furler, R.A. 1991. Angular dependence of optical properties of homogeneous glasses. *ASHRAE Transactions* 97(2):1129–33.

DOE. 2007. *EnergyPlus Engineering Reference—The Reference to EnergyPlus Calculations*. Washington, DC: U.S. Department of Energy.

Grasso, M., and D.R. Buchanan. 1979. Roller shade system effectiveness in space heating energy conservation. *ASHRAE Transactions* 85(2520):156–73.

Grasso, M., and D.R. Buchanan. 1982. Window shades in energy conservation. *Home Economics Research Journal* 11:89–97.

Harrison, S.J., and S.J. van Wonderen. 1998. Evaluation of solar heat gain coefficient for solar-control glazings and shading devices. *ASHRAE Transactions* 104(1b): 1051–62.

Keyes, M.W. 1967. Analysis and rating of drapery materials used for indoor shading. *ASHRAE Transactions* 73(1):8.4.1.

Kotey, N.A., M.R. Collins, J.L. Wright, and T. Jiang. 2008. A simplified method for calculating the effective solar optical properties of a venetian blind layer for building energy simulation. *ASME Journal of Solar Energy Engineering.* Forthcoming in the May issue.

Kotey, N.A., J.L. Wright, and M.R. Collins. 2009a. Determining off-normal solar optical properties of drapery fabrics. *ASHRAE Transactions* 115(1).

Kotey, N.A., J.L. Wright, and M.R. Collins. 2009b. Determining off-normal solar optical properties of insect screens. *ASHRAE Transactions* 115(1).

Look, D.C., Jr. 1986. Characteristics of a novel awning fabric. *Sun World* 10(4):117–20.

Ozisik, N., and L.F. Schutrum. 1959. Heat flow through glass with roller shades. *ASHRAE Transactions* 65(1696):697–716.

Parmelee, G.V., and W.W. Aubele. 1952. The shading of sunlit glass: An analysis of the effect of uniformly spaced flat opaque slats. *ASHVE Transactions* 58:377–98.

Pfrommer, P., K.J. Lomas, C. Seale, and Chr. Kupke. 1995. The radiation transfer through coated and tinted glazing. *Solar Energy* 54(5):287–99.

Pfrommer, P., K.J. Lomas, and Chr. Kupke. 1996. Solar radiation transport through slat-type blinds: A new model and its application for thermal simulation of buildings. *Solar Energy* 57(2):77–91.

Roos, A. 1997. Optical characterization of coated glazings at oblique angles of incidence: Measurements versus model calculations. *Journal of Non-Crystalline Solids* 218:247–55.

Rubin, M., K. Von Rottkay, and R. Powles. 1998. Models for the angle-dependent optical properties of coated glazing. *Solar Energy* 66(4):267–76.

Rubin, M., K. Von Rottkay, and R. Powles. 1999. Window optics. *Solar Energy* 62(3):149–61.

van Dijk, H., P. Kenny, and J. Goulding (eds). 2002. *WIS—Advanced Windows Information System Reference Manual*.

Wright, J.L., and N.A. Kotey. 2006. Solar absorption by each element in a glazing/shading layer array. *ASHRAE Transactions* 112(2):3–12.

Yahoda, D.S., and J.L. Wright. 2005. Methods for calculating the effective solar-optical properties of a venetian blind layer. *ASHRAE Transactions* 111(1): 572–86.